Reach Avoid Games with Output Observer Mixed Monotone Reachable Set Estimation

Andrew C. Frommer *, Suraj Raval †, and Yancy Diaz-Mercado ‡
University of Maryland, College Park, MD, 20742

We consider the problem of overestimating the reachable set of a partially observable dynamical agent with unknown disturbance dynamics. We use the framework of mixed-monotonicity to obtain a conservative estimate of the reachable set with respect to bounds on the uncertain dynamics. High-gain observers are used to produce states of the estimates and collapse the reachable set estimate error. Analysis shows that the reachable set estimate can be bounded through careful gain design. The results are validated in simulation and on a real ballistic dynamical systems. The results are used to show capture can be achieved by a team of slow pursuers against a fast evader in a reach-avoid game.

I. Introduction

Reach-Avoid (RA) games are a class of differential games in which an evader seeks to reach a specified target set while avoiding capture or interference by opposing players [1]. These games have applications in robotics, autonomous systems, defense, and surveillance, where agents must navigate complex, adversarial environments. In many RA game scenarios, it is critical for pursuers to anticipate the evader's future behavior to strategize effectively. In previous work, we show that a winning strategy for a team of slower pursuers in a time-bounded RA game is to position themselves to partition the evader's reachable set into disjoint subsets—one containing the evader and the other enclosing its goal [2]. By doing so, the pursuers can effectively block the evader's path to the target, forcing capture or running out the clock. Implementing this strategy, however, requires accurate computation or estimation of the evader's reachable set.

Mixed Monotone Reachable Set (MMRS) estimation has emerged as a powerful technique for efficiently computing conservative approximations of reachable sets for systems with bounded disturbances and uncertain inputs. Recent advancements, including the work in [3], [4] , have demonstrated how mixed monotone decomposition functions can be used to decompose a system's dynamics into cooperative and antagonistic components. This decomposition enables rapid and conservative reachable set estimation within hyperrectangular bounds, even for nonlinear systems. The application of MMRS estimation to RA games was explored in [5], where the MMRS framework was utilized to dynamically update the reachable set of the evader as its trajectory evolved. However, a significant limitation of this approach is its reliance on full-state information about the evader.

In many RA game settings, full-state measurements are not available. Instead, only partial state measurements, such as position, are available, with the remaining states, such as velocity, requiring estimation. In [5], velocity was estimated from prior measurements, but this introduced unmodeled errors that degraded the accuracy and conservativeness of the MMRS estimation. We address this limitation with an approach that incorporates partial-state observations into the MMRS framework while maintaining conservativeness.

High-gain observers (HGOs) provide a robust mechanism for estimating the full state of a system from partial state measurements [6]. HGOs have been deployed successfully for various nonlinear systems for partial as well as full state estimation [7–12]. HGOs leverage the separation between measurement dynamics and estimation dynamics to produce rapid and accurate state estimates, even in the presence of bounded disturbances. The inherent structure of HGOs also makes them well-suited for integration into conservative estimation frameworks, such as MMRS.

In this work, we synthesize a high-gain observer that estimates conservative upper and lower bounds on the state of a dynamical system, which can then be incorporated into MMRS estimation for RA games. By bounding the observer's estimation error within prescribed limits, we ensure that the MMRS remains a conservative approximation of the evader's true reachable set. Additionally, we derive conditions for the HGO's Lyapunov stability and demonstrate that these conditions are compatible with the requirements for MMRS estimation. Finally, we validate our approach in the

*PhD Student, Mechanical Engineering, Email: afromm88@umd.edu
†PhD Candidate, Mechanical Engineering, Email: sraval@umd.edu
‡Assistant Professor, Mechanical Engineering, Email: yancy@umd.edu

context of an RA game, illustrating that the proposed framework effectively supports pursuer strategies by enabling accurate and conservative estimation of the evader's reachable set based on partial-state information.

The structure of the paper is as follows: Section II introduces most of the notation followed throughout the paper. Section III introduces the framework of mixed-monotonicity to estimate reachable sets. We describe the reach-avoid game problem and reachable set estimation in Section IV. Analysis on the reachable set error is provided in Section V. We introduce the pursuer strategy in Section VI, validate the results in simulation in Section VII, and also provide hardware validation in Section VIII. Lastly, concluding remarks are provided in Section IX.

II. Notation

A vector $x \in \mathbb{R}^d$ will have components $x_1, ..., x_d \in \mathbb{R}$ and transpose $x^\top$. For vectors $x, y \in \mathbb{R}^d$, we say $x \prec y$ if $x_i < y_i$ for $i = 1, ..., d$. Given $x \prec y$ for $x, y \in \mathbb{R}^d$, the hyperrectangle $[[x, y]] = [x_1, y_1] \times \cdots \times [x_d, y_d]$. For $x, y \in \mathbb{R}^d$, let $(x, y) = [x^\top, y^\top]^\top \in \mathbb{R}^{2d}$. Furthermore, for $a = (x, y)$ we let $[[a]] = [[x, y]]$. We will let $\check{a}$ and $\hat{a}$ represent the lower and upper corners of a hypercube containing a. The notation a_e is used to represent an estimate of a. The notation x_{ev} and $x_{p,i}$ represents the evader state, and the state of the i^{th} pursuer.

III. Mixed-Monotonicity Preliminaries

As described in [3], consider the system

$$\dot{x} = F(x, w) \tag{1}$$

with state $x \in \mathcal{X} \subset \mathbb{R}^n$ and time-varying disturbance input $w(t) \in \mathcal{W} = [[\check{w}, \hat{w}]] \subset \mathbb{R}^m$ where the vector field F is locally Lipschitz continuous in its inputs, and that disturbance signals $w : \mathbb{R} \to \mathcal{W}$ is piece-wise continuous. The set of possible disturbances is a hyperrectangle.

Definition ([3]): Let $\mathcal{T} = \mathcal{X} \times \mathcal{W} \times \mathcal{X} \times \mathcal{W}$. Given a locally Lipschitz continuous function $d : \mathcal{T} \to \mathbb{R}^n$ the system (1) is *mixed-monotone with respect to d* if

- For all $x \in \mathcal{X}$ and all $w \in \mathcal{W}$ we have $d(x, w, x, w) = F(x, w)$.
- For all $i, j \in \{1, ..., n\}$, with $i \neq j$, we have $\frac{\partial d_i}{\partial \check{x}_j}(\check{x}, \check{w}, \hat{x}, \hat{w}) \geq 0$ for all $(\check{x}, \check{w}, \hat{x}, \hat{w}) \in \mathcal{T}$ such that $\frac{\partial d}{\partial \check{x}_j}$ exists.
- For all $i, j \in \{1, ..., n\}$, we have $\frac{\partial d_i}{\partial \hat{x}_j}(\check{x}, \check{w}, \hat{x}, \hat{w}) \leq 0$ for all $(\check{x}, \check{w}, \hat{x}, \hat{w}) \in \mathcal{T}$ such that $\frac{\partial d}{\partial \hat{x}_j}$ exists.
- For all $i \in \{1, ..., n\}$ and all $k \in \{1, ..., m\}$, we have $\frac{\partial d_i}{\partial \check{w}_k}(\check{x}, \check{w}, \hat{x}, \hat{w}) \geq 0 \geq \frac{\partial d_i}{\partial \hat{w}_k}(\check{x}, \check{w}, \hat{x}, \hat{w})$.

If (1) is mixed monotone with respect to d then d is called a *decomposition function* for (1).

We can use a mixed monotone decomposition to over-approximate the reachable set by constructing a deterministic embedding system. Given d,

$$\begin{bmatrix} \dot{\check{x}} \\ \dot{\hat{x}} \end{bmatrix} = E(\check{x}, \hat{x}) = \begin{bmatrix} d(\check{x}, \check{w}, \hat{x}, \hat{w}) \\ d(\hat{x}, \hat{w}, \check{x}, \check{w}) \end{bmatrix} \tag{2}$$

where we emphasize the order of the arguments. We refer to Eq. ((2)) as the *embedding system relative to d* and E the *embedding function relative to d*. We denote $\Phi^E(t, \check{x}_0, \hat{x}_0)$ the state of Eq. ((2)) reached at time t when beginning at state $\check{x}_0, \hat{x}_0 \in \mathcal{X}$ at time 0. For $0 < T < \infty$, we are interested in estimating the reachable set $\mathcal{R}([0, T]; \mathcal{X}_0) = \{x(T) \in \mathcal{X} \mid \dot{x}(t) = F(x(t), w(t)),\ t \in [0, T],\ x(0) \in \mathcal{X}_0\}$.

Proposition ([3]): Let Eq. ((1)) be mixed monotone with respect to d and consider $[[\check{x}_0, \hat{x}_0]] \subset \mathcal{X} \times \mathcal{X}$. If $\Phi^E(\tau, \check{x}_0, \hat{x}_0) \in \mathcal{X} \times \mathcal{X}$ for all $0 \leq \tau \leq t$, then $\mathcal{R}([0, t]; [[\check{x}_0, \hat{x}_0]]) \subseteq [[\Phi^E(t, \check{x}_0, \hat{x}_0)]]$.

In other words, the hyperrectangle constructed from the solution to Eq. ((2)) provides a conservative estimate of the true reachable set.

IV. Problem Definition

A. Reach Avoid Game

We consider the reach-avoid (RA) variant of a pursuit-evasion game, wherein a single evader attempts to travel to (reach) a goal set while avoiding a team of $N > 1$ coordinated pursuers. Due to finite energy budget considerations, we focus on finite-time games, where there exists an upper bound for game conclusion $T < \infty$. If the evader reaches its goal set before this time while avoiding capture, then it wins. Otherwise, the pursuers win.

B. Evader Reachable Set

Consider the evader dynamical system of the form

$$\begin{aligned} \dot{x} &= z \\ \dot{z} &= f(z, w) \\ y &= Cx + Dz \end{aligned} \tag{3}$$

where $w \in [[\check{w}, \hat{w}]] = \mathcal{W}$ is a disturbance that is contained in the hyperrectangle with corners $\check{w}$ and $\hat{w}$, y is the measured output, which is linear in the states $x, z \in \mathcal{X}$, and $f : \mathcal{X} \times \mathcal{W} \to \mathcal{X}$ is Lipschitz continuous. The initial conditions are assumed to be unknown, but bounded such that $x(0) \in [[\check{x}_0, \hat{x}_0]]$ and $z(0) \in [[\check{z}_0, \hat{z}_0]]$.

Using the framework of mixed-monotonicity, we note that

$$\mathcal{R}([t,T]; [[(\check{x}(t), \check{z}(t)), (\hat{x}(t), \hat{z}(t))]]) \subseteq [[(\check{x}(T), \check{z}(T)), (\hat{x}(T), \hat{z}(T))]],$$

where $\check{x}(T), \check{z}(T), \hat{x}(T)$, and $\hat{z}(T)$ are the solutions at time $t = T$ to the dynamics

$$\begin{aligned} \dot{\check{x}} &= \check{z} \\ \dot{\check{z}} &= d(\check{z}, \check{w}, \hat{z}, \hat{w}) \\ \dot{\hat{x}} &= \hat{z} \\ \dot{\hat{z}} &= d(\hat{z}, \hat{w}, \check{z}, \check{w}) \end{aligned} \tag{4}$$

with initial conditions $\check{x}_0, \hat{x}_0, \check{z}_0, \hat{z}_0 \in \mathcal{X}_0$, and d is a decomposition function to the dynamics for z.

Note that only the output $y = Cx + Dz$ is assumed to be measurable. We therefore produce an estimate of the states using the following high-gain observer design

$$\begin{aligned} \dot{\check{x}}_e &= \check{z}_e + Lg_1(y - \check{y}_e) \\ \dot{\check{z}}_e &= d(\check{z}_e, \check{w}, \hat{z}_e, \hat{w}) + L^2 g_2(y - \check{y}_e) \\ \dot{\hat{x}}_e &= \hat{z}_e + Lg_1(y - \hat{y}_e) \\ \dot{\hat{z}}_e &= d(\hat{z}_e, \hat{w}, \check{z}_e, \check{w}) + L^2 g_2(y - \hat{y}_e) \end{aligned} \tag{5}$$

Here, yet-to-be-defined, g_1, g_2 are gain matrices of appropriate dimensions, and $L > 0$ is a scalar observer gain to designed for stability.

V. Analysis of Reachable Set Error

We are interested in characterizing the size of the reachable set. We do so by evaluating the error between the containing hyperrectangle upper and lower corners. For $L > 0$, let

$$\xi = \begin{bmatrix} \xi_1 \\ \xi_2 \end{bmatrix} = \begin{bmatrix} L^{-1}(\hat{x}_e - \check{x}_e) \\ L^{-2}(\hat{z}_e - \check{z}_e) \end{bmatrix}$$

The error dynamics are thus

$$\begin{aligned} \dot{\xi} &= \begin{bmatrix} L^{-1}(\hat{z}_e - \check{z}_e) - g_1(\hat{y}_e - \check{y}_e) \\ L^{-2}(d(\hat{z}_e, \hat{w}, \check{z}_e, \check{w}) - d(\check{z}_e, \check{w}, \hat{z}_e, \hat{w})) - g_2(\hat{y}_e - \check{y}_e) \end{bmatrix} \\ &= -L \begin{bmatrix} G_{11} & (I + G_{12}) \\ G_{21} & G_{22} \end{bmatrix} \xi + L^{-2} \begin{bmatrix} 0 \\ d(\hat{z}_e, \hat{w}, \check{z}_e, \check{w}) - d(\check{z}_e, \check{w}, \hat{z}_e, \hat{w}) \end{bmatrix} \end{aligned}$$

where we used $\check{y}_e = C\check{x}_e + D\check{z}_e$, $\hat{y}_e = C\hat{x}_e + D\hat{z}_e$, and define

$$\begin{bmatrix} G_{11} & G_{12} \\ G_{21} & G_{22} \end{bmatrix} = \begin{bmatrix} g_1 C & g_1 D \\ g_2 C & g_2 D \end{bmatrix}$$

We design our gain matrices g_1 and g_2 such that

$$A = -\begin{bmatrix} G_{11} & (I + G_{12}) \\ G_{21} & G_{22} \end{bmatrix} \tag{6}$$

is Hurwitz. The error dynamics can then be written as

$$\dot{\xi} = LA\xi + L^{-2}(\tilde{d}(\hat{z}_e, \hat{w}, \check{z}_e, \check{w}) - \tilde{d}(\check{z}_e, \check{w}, \hat{z}_e, \hat{w})) \tag{7}$$

where

$$\tilde{d}(\check{x}.\check{w}, \hat{x}, \hat{w}) = (0, d(\check{x}.\check{w}, \hat{x}, \hat{w})) = \begin{bmatrix} 0 \\ d(\check{x}.\check{w}, \hat{x}, \hat{w}) \end{bmatrix}$$

It'll be convenient to define $P \succ 0$ to be the solution to

$$PA + A^\top P = -2I \tag{8}$$

and let $\lambda_P = \max_{x \neq 0}(x^\top Px)/(x^\top x)$. Further, as d is continuously differentiable, there exists a Lipschitz constant $K_d \geq \|Dd(x', w', x'', w'')\|_{\infty,\mathcal{T}}$, i.e., the Lipschitz constant is bounded below by the infinity norm of the total derivative for d for $x', x'' \in \mathcal{X}$ and $w', w'' \in \mathcal{W}$. We can now present our main result.

Theorem V.1. *For $L^3 > 2\lambda_P K_d$ the error dynamics $\dot{\xi}$ are Lyapunov stable with Lyapunov function $V(\xi) = \frac{1}{2}\xi^\top P\xi$, and the Lyapunov function is bounded by $W(t) = \frac{(b - e^{\frac{1}{2}a(t+c)})^2}{a^2}$ which is a solution to Eq. (20) with,*

$$a = 4L^{-2}K_d - 2L/\lambda_P \tag{9}$$

$$b = 2\sqrt{(2/(\lambda_P)}L^{-2}K_d\lambda_P(\|\overline{w} - \underline{w}\|) \tag{10}$$

Proof. Consider the candidate Lyapunov function

$$V(\xi) = \frac{1}{2}\xi^\top P\xi \leq \frac{1}{2}\lambda_P\|\xi\| \tag{11}$$

Taking the derivative yields

$$\begin{aligned} \dot{V}(\xi) &= 1/2\xi^\top P\dot{\xi} + \dot{\xi}^\top P\xi \\ &= \tfrac{L}{2}\xi^\top(A^\top P + AP)\xi + L^{-2}\xi^\top P(\tilde{d}(\check{z}_e, \overline{w}, \hat{z}_e, \underline{w}) - \tilde{d}(\check{z}_e, \underline{w}, \hat{z}_e, \overline{w})) \\ &= -L\|\xi\|^2 + L^{-2}\xi^\top P((\tilde{d}(\check{z}_e, \overline{w}, \hat{z}_e, \underline{w}) - \tilde{d}(\check{z}_e, \underline{w}, \hat{z}_e, \overline{w}))) \end{aligned} \tag{12}$$

We now need to bound $\xi^\top P(\tilde{d}(\check{z}_e, \overline{w}, \hat{z}_e, \underline{w}) - \tilde{d}(\check{z}_e, \underline{w}, \hat{z}_e, \overline{w}))$. By Cauchy-Schwarz

$$\begin{aligned} \xi^\top P((\tilde{d}(\check{z}_e, \overline{w}, \hat{z}_e, \underline{w}) - \tilde{d}(\check{z}_e, \underline{w}, \hat{z}_e, \overline{w}))) &\leq |\xi^\top P(\tilde{d}(\check{z}_e, \overline{w}, \hat{z}_e, \underline{w}) - \tilde{d}(\check{z}_e, \underline{w}, \hat{z}_e, \overline{w}))| \\ &\leq \sqrt{(\xi^\top P\xi)(\tilde{d}(\check{z}_e, \overline{w}, \hat{z}_e, \underline{w}) - \tilde{d}(\check{z}_e, \underline{w}, \hat{z}_e, \overline{w}))^\top P(\tilde{d}(\check{z}_e, \overline{w}, \hat{z}_e, \underline{w}) - \tilde{d}(\check{z}_e, \underline{w}, \hat{z}_e, \overline{w}))} \\ &\leq \lambda_P\|\xi\|\|(\tilde{d}(\check{z}_e, \overline{w}, \hat{z}_e, \underline{w}) - \tilde{d}(\check{z}_e, \underline{w}, \hat{z}_e, \overline{w}))\| \end{aligned} \tag{13}$$

From here consider $\|\tilde{d}(\check{z}_e, \overline{w}, \hat{z}_e, \underline{w}) - \tilde{d}(\check{z}_e, \underline{w}, \hat{z}_e, \overline{w})\|$. Since d is Lipschitz

$$\begin{aligned} \|\tilde{d}(\hat{z}, \overline{w}, \check{z}, \underline{w}) - \tilde{d}(\check{z}, \underline{w}, \hat{z}, \overline{w})\| &\leq K_d\|(\hat{z}, \overline{w}, \check{z}, \underline{w}) - (\check{z}, \underline{w}, \hat{z}, \overline{w})\| \\ &= K_d\sqrt{\|\hat{z} - \check{z}\|^2 + \|\overline{w} - \underline{w}\|^2 + \|\check{z} - \hat{z}\|^2 + \|\underline{w} - \overline{w}\|^2} \end{aligned} \tag{14}$$

By subadditivity of the square root

$$\begin{aligned} \|\tilde{d}(\hat{z}, \overline{w}, \check{z}, \underline{w}) - \tilde{d}(\check{z}, \underline{w}, \hat{z}, \overline{w})\| &\leq K_d(\|\hat{z} - \check{z}\| + \|\overline{w} - \underline{w}\| + \|\check{z} - \hat{z}\| + \|\underline{w} - \overline{w}\|) \\ &= 2K_d\|\hat{z} - \check{z}\| + 2K_d\|\overline{w} - \underline{w}\| \\ &= 2K_d\|\xi_2\| + 2K_d\|\overline{w} - \underline{w}\| \end{aligned} \tag{15}$$

So then the Lyapunov derivative is bounded by

$$\dot{V}(\xi) \leq -L\|\xi\|^2 + L^{-2}\lambda_P\|\xi\|(2K_d\|\xi_2\| + 2K_d\|\overline{w} - \underline{w}\|) \tag{16}$$

Because $\|\xi_2\| \leq \|\xi\|$, we get $\|\xi\|\|\xi_2\| \leq \|\xi\|^2$

$$\begin{aligned}\dot{V}(\xi) &\leq -L\|\xi\|^2 + 2K_dL^{-2}\lambda_P\|\xi\|^2 + 2K_dL^{-2}\lambda_P\|\overline{w} - \underline{w}\|\|\xi\| \\ &= (2L^{-2}K_D\lambda_P - L)\|\xi\|^2 + 2L^{-2}K_d\lambda_P\|\overline{w} - \underline{w}\|\|\xi\| \\ &\leq (4L^{-2}K_d - 2L/\lambda_P)V(\xi) + 2\sqrt{2/\lambda_P}L^{-2}K_d\lambda_P\|\overline{w} - \underline{w}\|\sqrt{V(\xi)}\end{aligned} \tag{17}$$

Let

$$a = 4L^{-2}K_d - 2L/\lambda_P \tag{18}$$

$$b = 2\sqrt{(2/(\lambda_P)}L^{-2}K_d\lambda_P(\|\overline{w} - \underline{w}\|) \tag{19}$$

The upper bound thus has the structure of the Bernoulli differential equation given by

$$\dot{W} = aW + b\sqrt{W} \tag{20}$$

Such an equation has solution

$$W(t) = \frac{(b - e^{\frac{1}{2}a(t+c)})^2}{a^2} \tag{21}$$

Where constant c is found by solving $W(0) = \frac{1}{2}\xi(0)^\top P\xi(0)$. By the comparison lemma, if $W(0) = V(0)$ and $\dot{V} \leq \dot{W}$ then $V(t) \leq W(t)$. Thus the Bernouli solution Eq. (21) provides an upper bound on the solution to the Lyapunov candidate function. For $a < 0$

$$\lim_{t\to\infty} V(t) = b^2/a^2 \tag{22}$$

Then $a < 0$ when $L^3 > 2\lambda_P K_d$, and the result follows. □

VI. Reachable Set and RA Game Strategy

A. Reachable Set

The observer dynamics are only meaningful for the instantaneous state. In order to estimate the RS we rely on the embedding system Eq. (2). Define an a pair of augmented state $\check{s}(t) = [y(t),\ \check{z}_e(t)]^\top$ and $\hat{s}(t) = [y(t),\ \hat{z}_e(t)]^\top$. Then the corners of the RS estimate hyperrectangle at some future time T_f are given by

$$[\check{s}^{T_f}(t),\ \hat{s}^{T_f}(t)]^\top = \Phi^E(T_f, \check{s}(t), \hat{s}(t)) \tag{23}$$

Note that this is a function of time because the observer states and measurements are constantly updated, so as new information about the system is gained, the forward reachable set is updated.

B. Reach Avoid Game

Consider the RA game setting presented in [5]. In this setting a team of embedded 2D planar agents attempts to coordinate to prevent a faster evader from reaching its goal by passing through their embedded plane. The evader dynamics are given by a three-dimensional ballistic trajectory with unknown aerodynamic forces

$$\begin{bmatrix}\dot{x}_{ev} \\ \dot{z}_{ev}\end{bmatrix} = \begin{bmatrix}z_{ev} \\ 1/m(-T||z_{ev}||z_{ev} + N(z_{ev} \times w) - mg\end{bmatrix} \tag{24}$$

$$y_{ev} = x_{ev} \tag{25}$$

Where the evader position is $x_{ev} \in \mathbb{R}^3$ is directly measurable, but the evader velocity given by $z_{ev} \in \mathbb{R}^3$ is not. The aerodynamic lift force is provided by an unknown spin given by $w \in \mathbb{R}^3$ such that $\underline{w} \preceq w \preceq \overline{w}$ and $\langle w, z_e v\rangle = 0$.

$T = \frac{1}{2}C_d\rho A$ is a constant associated with the drag force, $N = \frac{1}{2}C_l\rho r A$ is a constant associated with the lift force, m is the mass of the evader, and $g = [0,\ 0,\ 9.81]^\top$ is the gravitational constant. C_d and C_l are the drag and lift coefficients respectively, ρ is the air density, A is the ball cross-sectional area, and r the ball radius. The decomposition for Equation (24) is presented in [5].

In this game setting the pursuers are a team of homogeneous ground agents with single integrator dynamics

$$\dot{x}_{p,i} = u_{p,i} \tag{26}$$

where $x_{p,i} \in \mathbb{R}^3$ is the i^{th} agent's planar position embedded in $\mathbb{R}^3$, $i = 1, \ldots, N$. The velocity of the pursuers are bounded, such that $\|u_{p,i}\| \in [0, z_p]$. The evaders maximum velocity is known to be significantly greater than that of the pursuers, i.e., $v_{ev} \gg v_p$. Capture is defined as any member of the pursuer team coming within ϵ (the capture radius) of the evader, such that

$$\|x_{p,i} - x_{ev}\|_2 \leq \epsilon$$

the Euclidean distance between the evader position in $\mathbb{R}^3$ and the planar position of the pursuer embedded in $\mathbb{R}^3$.

The pursuers attempt to separate the evader from its goal by distributing themselves on the intersection of their embedding plane with the evader's reachable set according to the strategy in [5]. Each evader is associated with a virtual agent, which performs coverage control [13] over the intersection of the embedding plane with the evader's RS estimate. The slow evaders then track the virtual pursuer at maximum speed until either the evader is captured or passes through the embedding plane. Using virtual agents allows pursuers who have exited the evader RS to continue to participate in the game in case there is a possibility that they may re-enter the RS before the conclusion of the game.

VII. Simulation Results

A. Observer

To validate the performance of such an observer we the RA games with evader dynamics provided by Eq. (24), in this simulation, the initial position $y_{ev}(0)$ is assumed known. Additionally the initial velocity $z_{ev}(0) \in \mathbb{R}^3$ is bounded by $z_{ev} \in [[\check{z}(0),\ \hat{z}(0)]]$. For the purpose of validating the observer, the true aerodynamic disturbance $w \in \mathbb{R}^3$ is used to compute the true dynamics and state but the observer only uses bounds on the aerodynamic disturbance $\check{w}, \hat{w}$ and the embedding system for the observer. The observer estimates are initialized by the known initial positions and velocity bounds as

$$\begin{aligned}
\check{x}_e(0) &= y(0) \\
\check{z}_e(0) &= \check{z}(0) \\
\hat{x}_e(0) &= y(0) \\
\hat{z}_e(0) &= \hat{z}(0).
\end{aligned}$$

We have provided a number of visualizations to demonstrate the performance of the observer. In Fig. 1 we show how each component of the estimates evolves with time demonstrating how the upper and lower estimates of both x_{ev} and z_{ev} are framed the estimates. In Fig. 2 we show three snapshots in time of the three dimensional trajectory along with the forward estimated reachable set at each time. As the observer more accurately estimates the velocity, the RS estimate shrinks. In Fig. 3 we compare the solution Eq. (21) to the solution of the actual Lyapunov function, Eq. (11).

B. Lipschitz Continuity for Evader Dynamics

Note that the condition for Lyapunov stability derived in previous sections depends on choosing the gain L that satisfies $L^3 \geq 2\lambda_p K_d$. It necessitates finding the Lipschitz constant K_d for the evader's decomposition function. We find the value of K_d by evaluating the ∞-norm of the Jacobian of $d(\check{z}_e, \underline{w}, \hat{z}_e, \overline{w})$. We do so by constructing a function which outputs the ∞-norm of the state-dependent Jacobian. The MATLAB function 'fmincon' is used for the optimization over the state-space. We find $K_d = 0.0292$ from this process, which governs the choices of gains for simulation as well as experiments.

C. Reach Avoid Game

Additionally, in the same testbed, we simulate the reach avoid game described in VI.B. Using the observer presented in this work as well as the pursuer strategy outlined in [5], we demonstrate that the pursuers are able to coordinate their

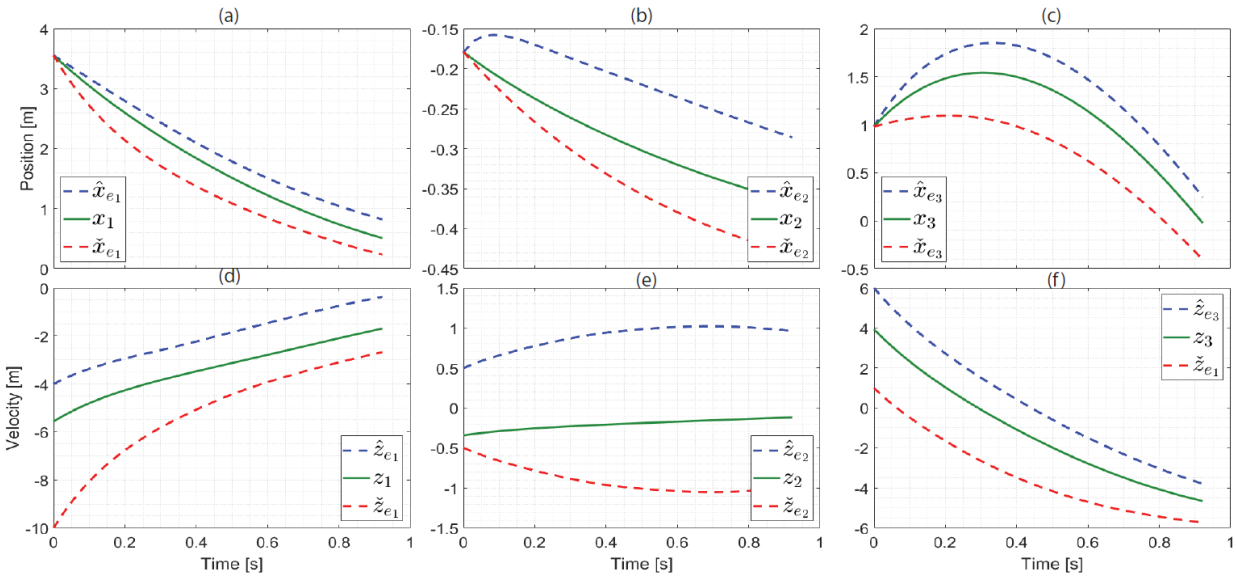

Fig. 1 Illustrates simulation plots (a) Evolution of the X position estimate from the observer ($\check{x}_{e_1}, \hat{x}_{e_1}$) compared to the true state (x_1). (b) and (c) illustrate the corresponding evolution for the Y and Z position components, respectively. (d) Evolution of the X velocity estimate from the observer ($\check{z}_{e_1}, \hat{z}_{e_1}$). (e) and (f) depict the respective evolution of Y and Z velocity components.

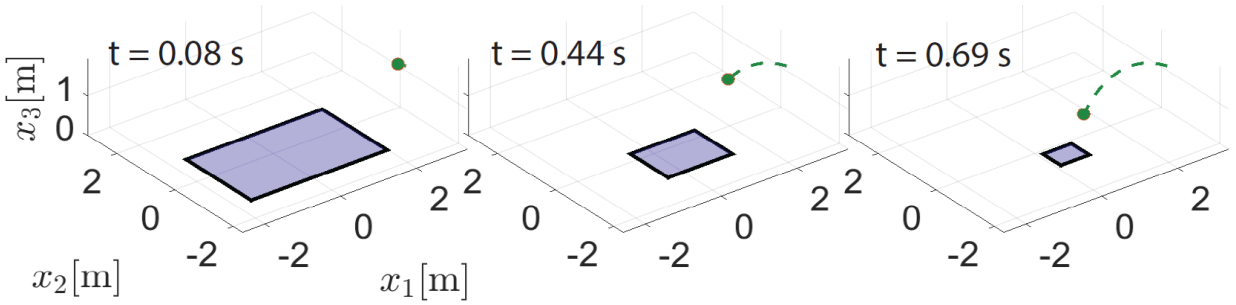

Fig. 2 Snapshots of simulation showing the evader's trajectory and its corresponding MMRS (purple patch) at the indicated times (from left to right) respectively.

motion and separate the evader from its goal.

VIII. Hardware Validation

In addition to simulating the system to validate the observer, and reachable set estimation, we also implement the observer on a real testbed. In our experiment, the evader is a foam ball that is launched from a toy ball launcher with an unknown speed (but with known bounds). At launch, the launcher imparts spin of unknown angular velocity that in turn generates unknown lift. The dynamics of the evader are assumed the same as the simulation (given in Eq. (24)). Parameters such as T, N, C_d, C_l are calculated in the same manner as done in Section VI.

The data were collected using a Vicon motion capture system, which recorded the evader's (ball) position throughout its trajectory. The observer design and RS estimation were implemented in real-time, utilizing the position estimates provided by the Vicon system. Figures 7 and 8 offer a detailed view of the experimental setup and its implementation. Figures 5 and 6 provide enhanced visualization and insights into the experimental data. A comparison between these experimental results and the simulation reveals a strong agreement, demonstrating the consistency between the two.

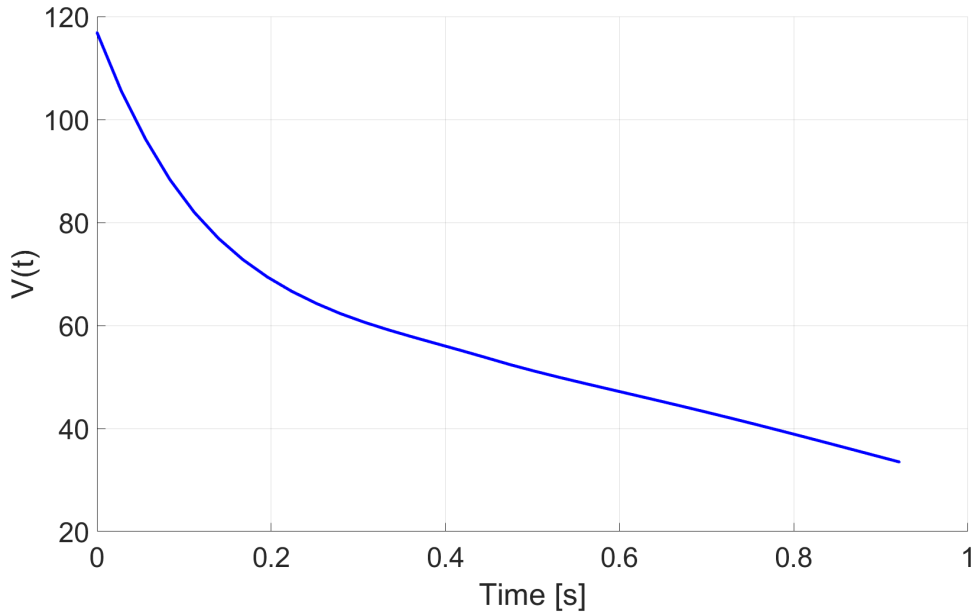

Fig. 3 The plot illustrates the temporal evolution of the Lyapunov function $V(t)$ for the entire trajectory of our simulation.

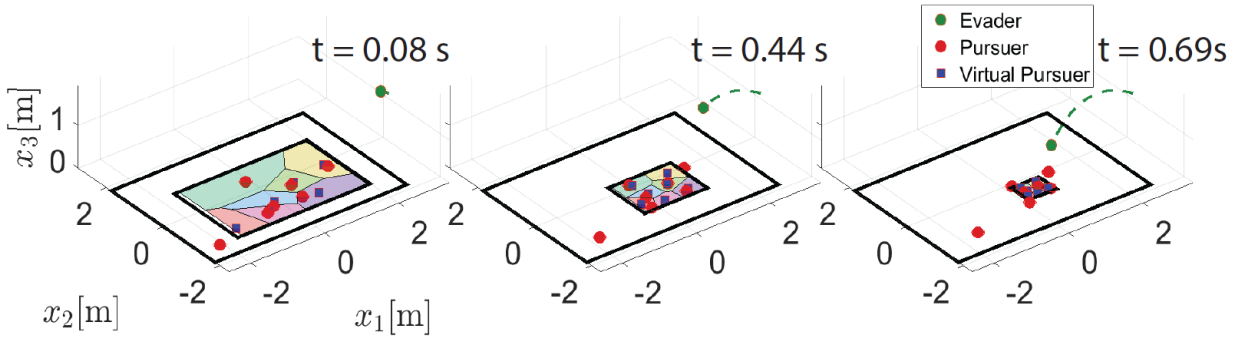

Fig. 4 Snapshots of simulation showing the evader's trajectory and its corresponding MMRS (purple patch) at the indicated times (from left to right) respectively. Additionally, the figure also shows the pursuers' (virtual as well as real) positions at these time instants.

IX. Conclusions

This work introduces a framework for estimating the reachable set of a partially observable dynamical system with bounded uncertainties, leveraging mixed monotonicity theory and high-gain observers. The proposed approach provides a conservative method for bounding the reachable set. Furthermore, we derived conditions ensuring the Lyapunov stability of the error dynamics. To validate the proposed methodology, we present both simulation results and hardware implementations that demonstrate the effectiveness of this approach in estimating reachable sets. We also demonstrate, through simulation, the application of this method for estimating the reachable set of an evader and its integration into a pursuer strategy within a reach-avoid game framework. Future work includes reasoning about the observer error and implementing the reach avoid game on hardware.

Appendix

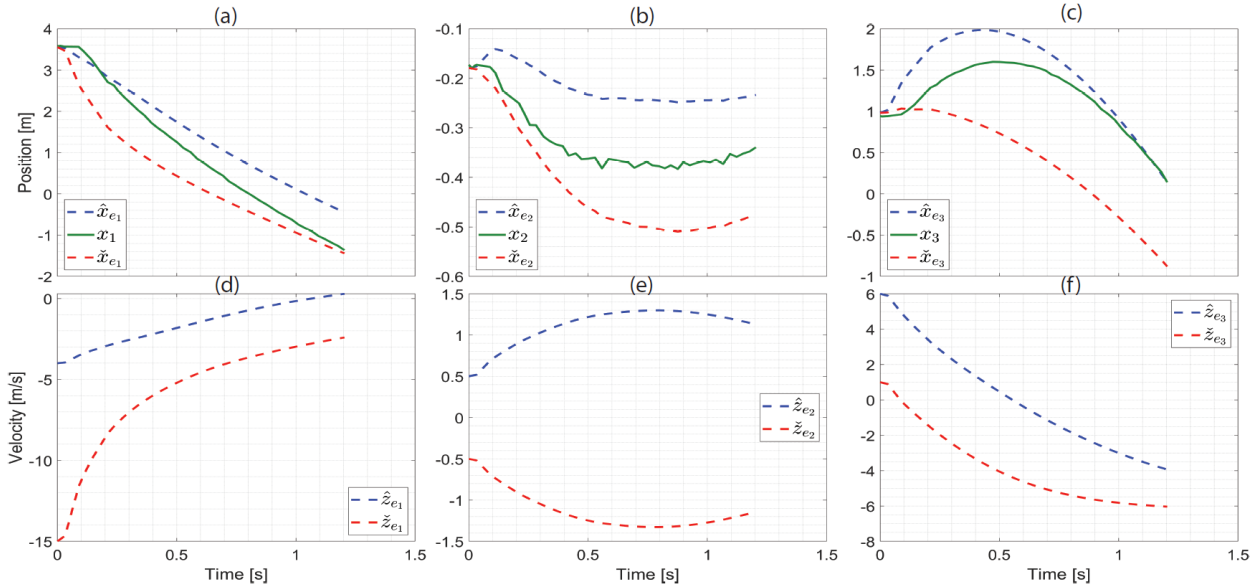

Fig. 5 **Illustrates experimental plots (a) Evolution of the x component of the position estimate from the observer ($\check{x}_{e_1}, \hat{x}_{e_1}$) compared to the measured state (x_1). (b) and (c) illustrate the corresponding evolution for the y and z position components, respectively. (d) Evolution of the x component of velocity estimate from the observer ($\check{z}_{e_1}, \hat{z}_{e_1}$). (e) and (f) depict the respective evolution of y and z velocity components.**

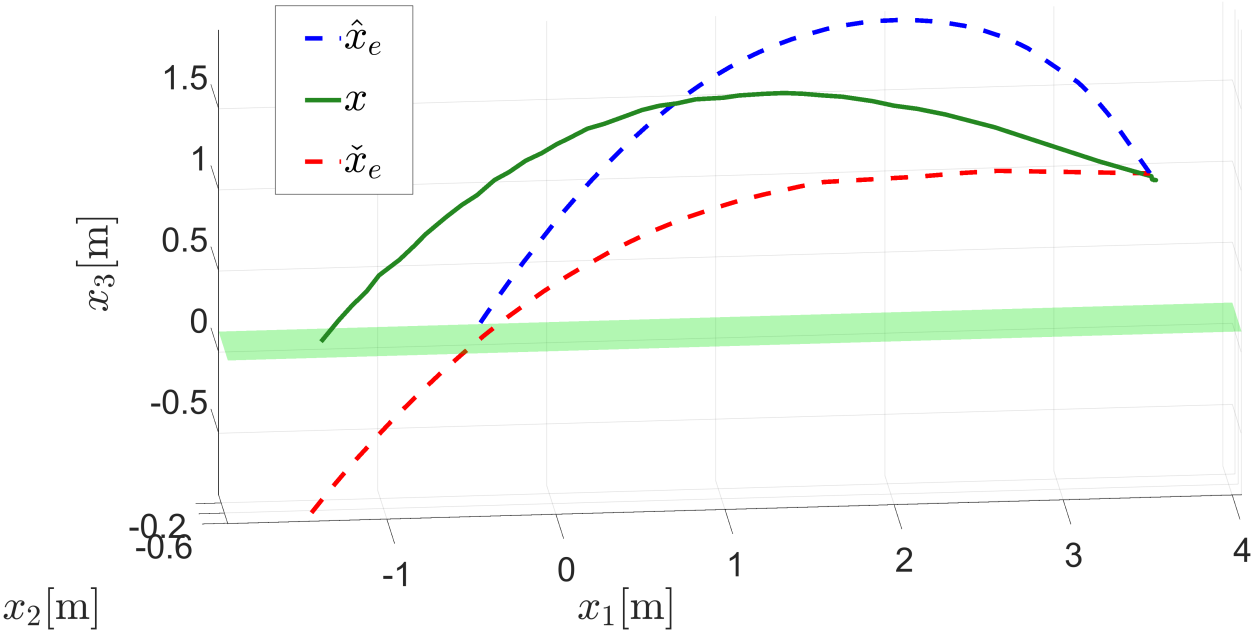

Fig. 6 **Illustrates experimental plots. Evolution of the position estimate from the observer ($\check{x}_e, \hat{x}_e$) compared to the measured state (x) in 3D space for the entire trajectory. The green plane represents the ground.**

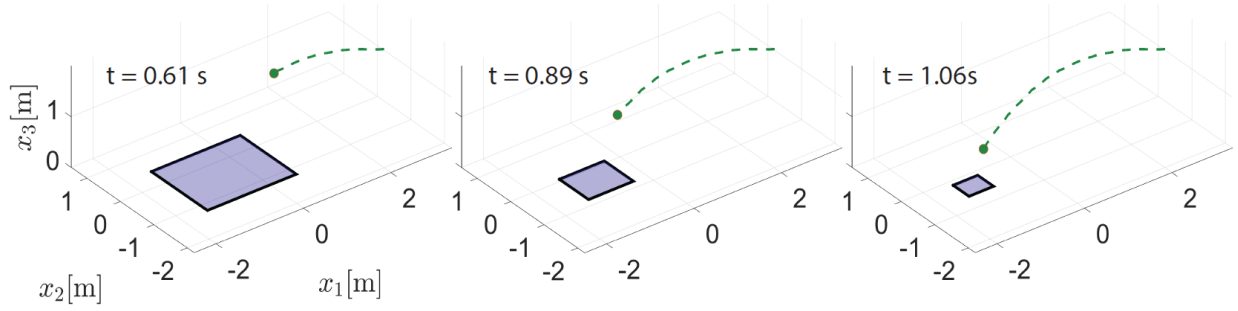

Fig. 7 Replay of the experimental data at various time instants, with the purple patch indicating the MMRS of the evader at each corresponding time instant.

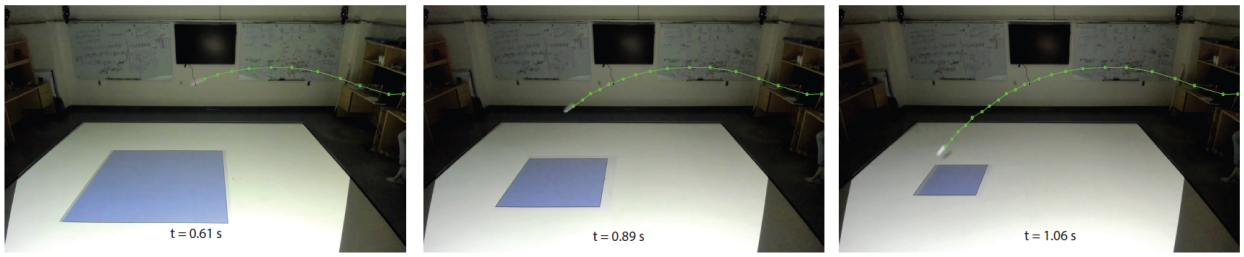

Fig. 8 Snapshots from the recorded experiments, illustrating the evader's trajectory and the corresponding MMRS plane projected onto the ground at specific time instants.

Table 1 Parameter Values in Simulation and Experiments

Parameter	Parameter Name	Simulation	Experiments
L	Observer Gain	1	1
G_1	Positional Gain Matrix	diag(3, 10, 3)	diag(3, 10, 3)
G_2	Velocity Gain Matrix	I_3	I_3
K_d	Lipschitz Constant	0.0292	0.0292
λ_P	Maximum Eigenvalue of P	10.299	10.299
r	Ball Radius	0.04 m	0.04 m
A	Ball Area	.05 m^2	0.05 m^2
C_d	Drag Co-efficient	0.405	0.405
C_l	Lift Co-efficient	0.62	0.62
$\underline{w}$	Spin Lower Bound	$[0,\ 0,\ -15]^\top$ rad/s	$[0,\ 0,\ -15]^\top$ rad/s
$\overline{w}$	Spin Lower Bound	$[0,\ 30,\ 15]^\top$ rad/s	$[0,\ 30,\ 15]^\top$ rad/s
v_i	Pursuer Maximum Velocity	1 m/s	×

Acknowledgments

This material is based upon research supported by, or in part by, the U.S. Office of Naval Research under award number N00014-21-1-2410.

References

[1] Zhou, Z., Takei, R., Huang, H., and Tomlin, C. J., "A general, open-loop formulation for reach-avoid games," *2012 IEEE 51st IEEE conference on decision and control (CDC)*, IEEE, 2012, pp. 6501–6506.

[2] Rivera, P., Kobilarov, M., and Diaz-Mercado, Y., "Pursuer coordination against a fast evader via coverage control," *IEEE Transactions on Automatic Control*, Vol. 69, No. 2, 2023, pp. 1119–1124.

[3] Abate, M., Dutreix, M., and Coogan, S., "Tight Decomposition Functions for Continuous-Time Mixed-Monotone Systems With Disturbances," *IEEE Control Systems Letters*, Vol. 5, No. 1, 2021, pp. 139–144. https://doi.org/10.1109/LCSYS.2020.3001085.

[4] Coogan, S., "Mixed Monotonicity for Reachability and Safety in Dynamical Systems," *2020 59th IEEE Conference on Decision and Control (CDC)*, 2020, pp. 5074–5085. https://doi.org/10.1109/CDC42340.2020.9304391.

[5] Frommer, A. C., Abate, M., Rivera-Ortiz, P. M., and Diaz-Mercado, Y., "A Capture Strategy for Multi-Pursuer Coordination Against a Fast Evader in 3D Reach-Avoid Games," *IFAC-PapersOnLine*, Vol. 56, No. 3, 2023, pp. 217–222. https://doi.org/https://doi.org/10.1016/j.ifacol.2023.12.027, URL https://www.sciencedirect.com/science/article/pii/S2405896323023601, 3rd Modeling, Estimation and Control Conference MECC 2023.

[6] Gauthier, J.-P., Hammouri, H., and Othman, S., "A simple observer for nonlinear systems applications to bioreactors," *IEEE Transactions on automatic control*, Vol. 37, No. 6, 1992, pp. 875–880.

[7] Arcese, L., Fruchard, M., and Ferreira, A., "Adaptive Controller and Observer for a Magnetic Microrobot," *IEEE Transactions on Robotics*, Vol. 29, No. 4, 2013, pp. 1060–1067. https://doi.org/10.1109/TRO.2013.2257581.

[8] Khalil, H. K., and Praly, L., "High-gain observers in nonlinear feedback control," *International Journal of Robust and Nonlinear Control*, Vol. 24, No. 6, 2014, pp. 993–1015.

[9] Crassidis, J. L., Markley, F. L., and Cheng, Y., "Survey of nonlinear attitude estimation methods," *Journal of guidance, control, and dynamics*, Vol. 30, No. 1, 2007, pp. 12–28.

[10] Ciccarella, G., Dalla Mora, M., and Germani, A., "A Luenberger-like observer for nonlinear systems," *International Journal of Control*, Vol. 57, No. 3, 1993, pp. 537–556.

[11] Gauthier, J.-P., and Kupka, I. A., "Observability and observers for nonlinear systems," *SIAM journal on control and optimization*, Vol. 32, No. 4, 1994, pp. 975–994.

[12] Prasov, A. A., and Khalil, H. K., "A nonlinear high-gain observer for systems with measurement noise in a feedback control framework," *IEEE Transactions on Automatic Control*, Vol. 58, No. 3, 2012, pp. 569–580.

[13] Cortes, J., Martinez, S., Karatas, T., and Bullo, F., "Coverage control for mobile sensing networks," *IEEE Transactions on Robotics and Automation*, Vol. 20, No. 2, 2004, pp. 243–255. https://doi.org/10.1109/TRA.2004.824698.